Neoplasia 57 (2024) 101036

Contents lists available at ScienceDirect

Neoplasia

journal homepage: www.elsevier.com/locate/neo

Original Research

Characterization of circulating tumor cells in patients with metastatic bladder cancer utilizing functionalized microfluidics

Zeqi Niu [a,b,h], Molly Kozminsky [a,b,h], Kathleen C. Day [c,h], Luke J. Broses [c,h], Marian L. Henderson [e,h], Christopher Patsalis [e,f,h], Rebecca Tagett [g], Zhaoping Qin [d], Sarah Blumberg [a,h], Zachery R. Reichert [e,h], Sofia D. Merajver [e,h], Aaron M. Udager [d,h], Phillip L. Palmbos [e,h], Sunitha Nagrath [a,b,h,**], Mark L. Day [c,h,*]

[a] Department of Chemical Engineering, University of Michigan, Ann Arbor, MI 48109, USA
[b] Biointerface Institute, University of Michigan, Ann Arbor, MI 48109, USA
[c] Department of Urology, University of Michigan, Ann Arbor, MI 48109, USA
[d] Department of Pathology, University of Michigan, Ann Arbor, MI 48109, USA
[e] Department of Internal Medicine, Hematology Oncology Division, University of Michigan, Ann Arbor, MI 48109, USA
[f] Department of Computational Medicine and Bioinformatics, University of Michigan, Ann Arbor, MI 48109, USA
[g] Bioinformatics Core, Michigan Medicine, University of Michigan, Ann Arbor, MI, USA
[h] Rogel Comprehensive Cancer Center, University of Michigan, Ann Arbor, MI 48109, USA

ARTICLE INFO

Keywords:
Circulating tumor cells
Bladder cancer
Targeted transcriptome sequencing
Differential gene expression
Graphene oxide microfluidic chip
ADAM15
CD31
EGFR
HER2

ABSTRACT

Assessing the molecular profiles of bladder cancer (BC) from patients with locally advanced or metastatic disease provides valuable insights, such as identification of invasive markers, to guide personalized treatment. Currently, most molecular profiling of BC is based on highly invasive biopsy or transurethral tumor resection. Liquid biopsy takes advantage of less-invasive procedures to longitudinally profile disease. Circulating tumor cells (CTCs) isolated from blood are one of the key analytes of liquid biopsy. In this study, we developed a protein and mRNA co-analysis workflow for BC CTCs utilizing the graphene oxide (GO) microfluidic chip. The GO chip was conjugated with antibodies against both EpCAM and EGFR to isolate CTCs from 1 mL of blood drawn from BC patients. Following CTC capture, protein and mRNA were analyzed using immunofluorescent staining and ion-torrent-based whole transcriptome sequencing, respectively. Elevated CTC counts were significantly associated with patient disease status at the time of blood draw. We found a count greater than 2.5 CTCs per mL was associated with shorter overall survival. The invasive markers EGFR, HER2, CD31, and ADAM15 were detected in CTC subpopulations. Whole transcriptome sequencing showed distinct RNA expression profiles from patients with or without tumor burden at the time of blood draw. In patients with advanced metastatic disease, we found significant upregulation of metastasis-related and chemotherapy-resistant genes. This methodology demonstrates the capability of GO chip-based assays to identify tumor-related RNA signatures, highlighting the prognostic potential of CTCs in metastatic BC patients.

Introduction

Every year, 600,000 people are diagnosed with bladder cancer (BC) worldwide, and >200,000 people die from this disease [1]. In the United States, over 82,000 patients were diagnosed with BC in 2023, with 25 % of these patients having muscle-invasive bladder cancer (MIBC) [2]. First-line treatment for MIBC patients includes neoadjuvant chemotherapy and radical cystectomy or radiation. Yet, half of these patients will relapse following therapy, with many patients diagnosed with metastasis [3]. The five-year survival for metastatic BC patients is only 6 %. Standard of care treatments for these metastatic patients include cisplatin-based chemotherapy, checkpoint inhibitor immunotherapy,

Abbreviations: BC, bladder cancer; CTCs, circulating tumor cells; FFPE, formalin fixed paraffin embedded; GO, graphene oxide; MIBC, muscle invasive bladder cancer; WBC, white blood cells; DEGs, differentially expressed genes.

* Corresponding author at: Department of Urology, Rogel Cancer Center University of Michigan, USA.
** Co-corresponding author at: Department of Chemical Engineering, University of Michigan, Ann Arbor,MI 48109, USA.
E-mail addresses: snagrath@umich.edu (S. Nagrath), mday@umich.edu (M.L. Day).

https://doi.org/10.1016/j.neo.2024.101036
Received 7 June 2024; Received in revised form 19 July 2024; Accepted 28 July 2024

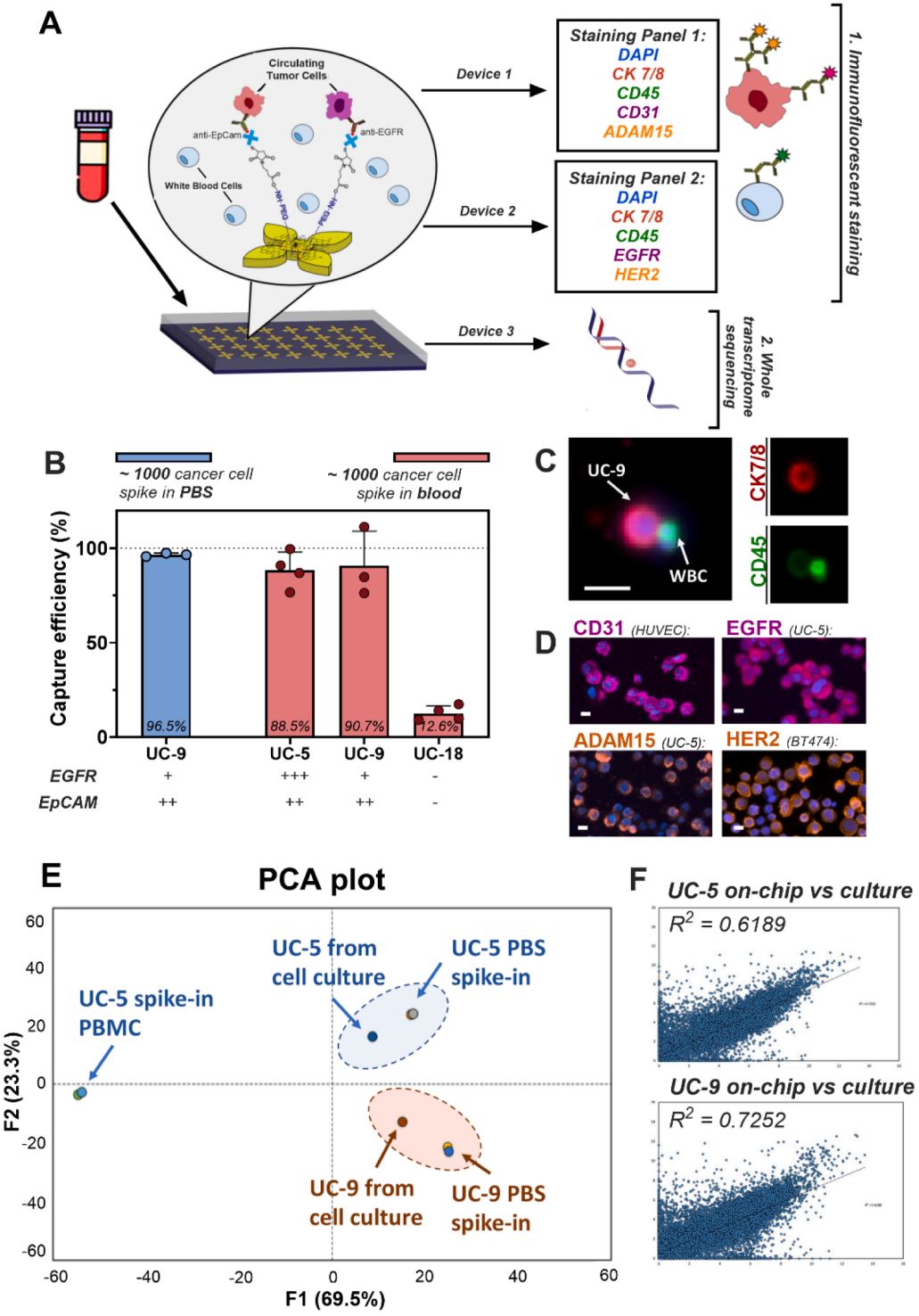

Fig. 1. Workflow optimization using cell line controls. (A) Schematic of the GO chip workflow. (B) Capture efficiency of bladder cancer cells spiked into PBS or healthy control blood samples. (C) Staining optimization of Cytokeratin 7/8 (CK 7/8) and CD45 using blood sample spiked with UC-9. (D) Examples of CD31, EGFR, ADAM15, and HER2 staining with corresponding cell lines. (E) Principal component analysis (PCA) of the RNA expression profile of UC-5 and UC-9 spike-in model samples in PBS and peripheral blood (PBMC), as well as expression profile from RNA extracted from culture. (F) Linear correlation of the expression between the UC-5 and UC-8 samples and the culture samples.

antibody drug conjugate therapy, and targeted therapy, such as Erdafitinib. However, most develop resistance to therapy. Molecular heterogeneity may be a driving factor in differential responses and drug resistance, thus contributing to patient mortality [4]. Molecular profiling of MIBC within The Cancer Genome Atlas (TCGA) BC cohort has revealed five widely accepted molecular subtypes (i.e., Luminal, Luminal papillary, Luminal infiltrated, Basal squamous, and neuroendocrine) which have differing overall survival and may require different treatment strategies [5]. Significant work has been done to identify predictive biomarkers for response to treatment modalities. Therefore, real-time molecular profiling of advanced BC can enable personalized disease care and guide appropriate therapeutic design throughout

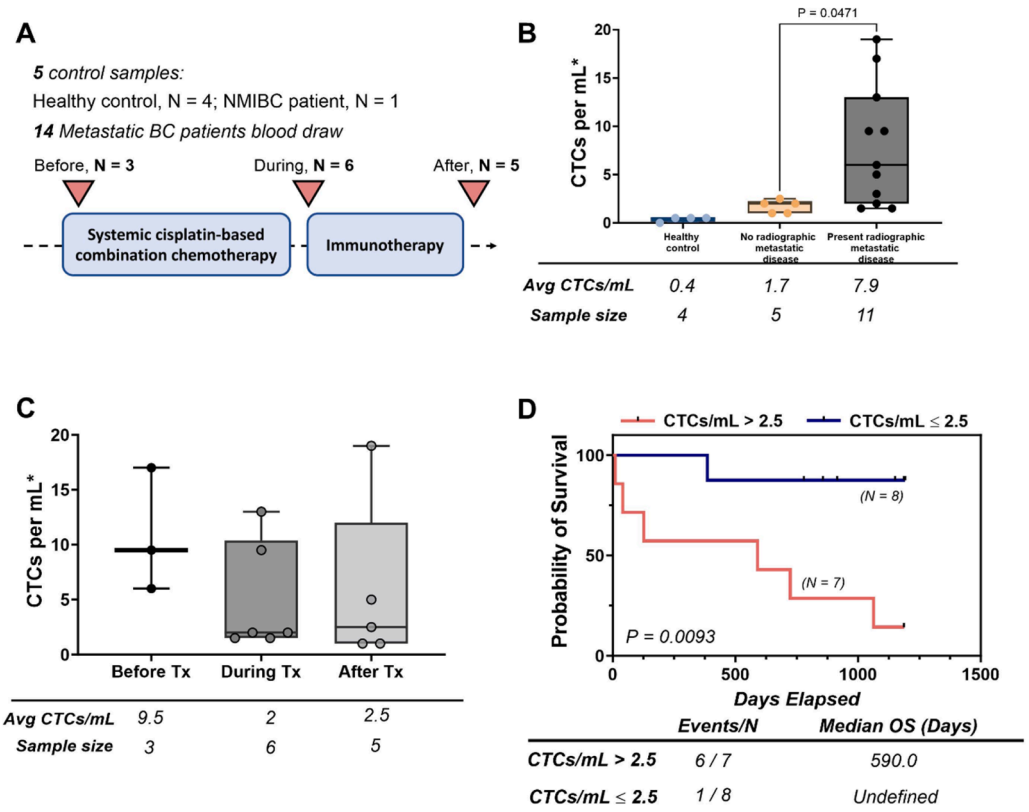

Fig. 2. CTC enumeration by EGFR/EpCAM capture in a cohort of metastatic muscle-invasive bladder cancer patients. (A) Study overview. (B) CTCs per mL in blood draws from healthy control, patients with no radiographic evidence of disease, or patients with present radiographic metastatic disease. (C) CTCs per mL from patient blood draws before, during, and after chemotherapy and immunotherapy. (D) Kaplan-Meier curve of CTCs greater or <2.5 CTCs/mL. *CTCs per mL on the y-axis is calculated by averaging the two immunofluorescent staining devices.

treatment progression.

Traditional tissue-based molecular profiling is limited by invasive tissue retrieval, resulting in few samples and the inability to monitor tumor evolution and response to therapy in real-time. In contrast, liquid biopsies have the potential to retrieve molecular information about the tumor through less invasive methods such as blood draws and urine collection during treatment. Circulating tumor cells (CTCs) are an important analyte of liquid biopsy. As the seeds of metastasis, these tumor cells in the circulation represent a promising prognostic biomarker in different cancer types [6–8]. CTCs in early-stage BC are associated with a higher risk for tumor recurrence and progression to muscle-invasive disease [9]. Further, the dynamic changes of CTCs in metastatic patients during chemotherapy are predicative of three-year progression-free survival (PFS) and overall survival (OS) [10].

Profiling of CTCs in BC has previously been limited by several factors. Most CTC studies in BC utilize the CellSearch^{TM} platform, an FDA-approved CTC isolation approach. This technology uses magnetic beads conjugated to antibodies against epithelial cell adhesion molecule (EpCAM) for CTC isolation. Immunoaffinity-based microfluidic devices use similar principles, but by conjugating antibodies against *additional* surface proteins, they provide a more versatile capturing capability of viable CTCs from small volumes of whole blood [11,12]. Previously, we developed a graphene oxide nanosheet-based microfluidic device (GO device) [13,14], successfully isolating CTCs from breast [15], lung [6], and prostate [16–18] cancer patients with high purity and sensitivity. The GO device captures CTCs using a near-flat nanostructure patterned on a silicon wafer substrate, making it an ideal platform for downstream immunofluorescence and RNA profiling.

Immunofluorescent staining of CTC proteins can be used to infer tumor characteristics. In BC, high concordance of HER2 status was found between primary tumors, CTCs, and lymph node metastasis, suggesting CTC-based testing could identify candidates for anti-HER2 therapy [19,20]. In addition, PD-L1 positive CTCs are found to be associated with worse overall survival [21]. Herein, we investigated the role of ADAM15, CK7/8, CD31, EGFR, and HER2 expression in BC CTCs to determine if BC CTCs expressed these biomarkers (**Table S1**). ADAM15, a type I transmembrane glycoprotein, is involved in cell adhesion and metastasis by modulating tumor-endothelial cell interaction [22,23]. CD31 (PECAM-1) is commonly used to identify vascular endothelial cells. CD31 positive CTCs, or circulating tumor-endothelial cells (CTECs), are generated through cell-fusion or trans-differentiation, and have hybridized properties of vascularization and motility [24]. Extensive research has shown that the ErbB family of receptor tyrosine kinases are associated with cancer metastasis [16]. We previously reported that EGFR over-expression is associated with prostate cancer bone metastasis, and is highly expressed on prostate cancer CTCs in metastatic disease [18]. In BC, the over-expression of EGFR and HER2 are positively correlated to the clinical stage, pathologic grade, and tumor recurrence [25]. Circulating tumor cell-based EGFR and HER2 profiling could thus, be utilized to screen patients for targeted therapies [26]. CK7 and CK8 (cytokeratins) are epithelial markers expressed in genitourinary systems, specifically for bladder cancer analysis [19,27,28].

Targeted real-time PCR (RT-PCR) is used to evaluate specific gene expression in RNA samples extracted from bladder CTC samples. Previously, KRAS, EpCAM, CD133, Survivin, PI3K, VEGF, mTOR, and AKT genes were found to have significantly increased expression in CTC-enriched samples [29]. In another study investigating colon cancer and BC patients, the high expression of EGFR and Tenascin C (TNC) from RNAs extracted from blood samples indicated worse clinical outcome [30]. However, RT-PCR is often conducted with limited gene panels while other technologies, such as next-generation RNA sequencing and single cell sequencing provide broader transcriptomic landscapes. One

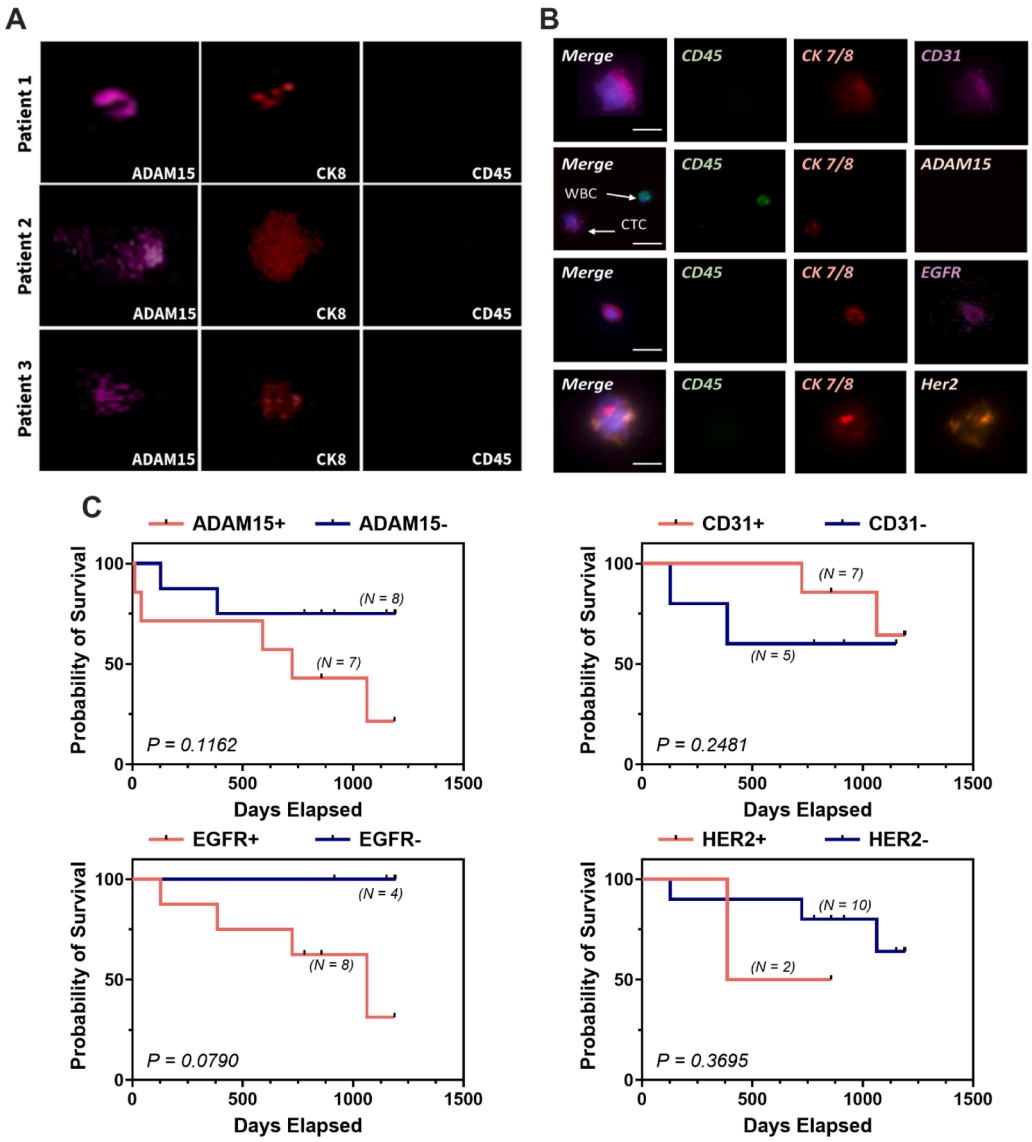

Fig. 3. Expression of invasive markers on bladder cancer patient CTCs. (A) Immunofluorescent images of CTCs highlighting ADAM15 from three patients with metastatic relapse. (B) Immunofluorescent images of CTCs with invasive marker expressions from a single MIBC patient. (C) Kaplan-Meier curves of patients with or without single invasive marker present.

of the difficulties for implementing these high-throughput molecular profiling technologies for CTCs is their apoptotic nature and low RNA quality and quantity. In FFPE tissue samples with similar low RNA quality and quantity, amplicon-based targeted RNA sequencing technology has been used to profile with consistent success [17].

In this proof-of-concept study, we established a two-fold analysis of BC CTCs; first, EGFR and EpCAM immunoaffinity CTC capture and immunofluorescent staining, and secondly, whole transcriptome sequencing. To begin, we utilized BC cell lines to optimize capture efficiency and molecular characterization. Subsequently, blood samples from patients were processed in triplicate using the GO platform (Fig. 1**A**). We developed a two-fold workflow whereby two of these devices were utilized for antibody staining, and the third device was used to isolate RNA for whole transcriptome sequencing. Using this workflow, we were able to identify biomarkers with prognostic potential on CTCs, as well as unveil the gene expression signatures of these patients.

Results

CTC isolation and optimization of the GO microfluidic chip

First, to test the capture efficiencies of the modified GO chip coupled with anti-EGFR and anti-EpCAM, we spiked human bladder cancer cell lines (UM-UC9, UM-UC5, or UM-UC18) into PBS or healthy control blood. In Fig. 1**B**, the capture efficiencies of UM-UC-5 and UM-UC-9 were over 88 % from both PBS and blood. As expected, capture required the expression of either EGFR or EpCAM. Only 12.8 % of UM-UC-18 cells were captured on this platform, as this cell line expresses low EGFR and low EpCAM (Western data not shown). To further differentiate CTCs from non-specifically bound WBCs, CTCs were stained for cytokeratin 7/8 (CK7/8, epithelial marker) and CD45 (WBC marker) [31]. Identified CK7/8 positive and CD45-negative CTCs were further evaluated for expression of ADAM15, CD31, EGFR, and HER2. Examples of positive control staining images of these markers are shown in Fig. 1**C, D**.

Secondly, we validated that amplicon-based whole transcriptome sequencing could accurately be accomplished and truly represent the

RNA expression profile following GO chip isolation. To do this, we compared expression profiles from UM-UC-5 and UM-UC-9 captured on chip to the RNA seq profile of UM-UC-5 and UM-UC-9 from cultured conditions. As shown in Fig. 1**E**, expression data from the same cell lines clustered together in the principal component analysis (PCA). The expression profiles of cell lines of the same origin between on-chip or from culture, positively correlated (Fig. 1**F**, UM-UC-5: $R^2 = 0.6189$; UM-UC-9: $R^2 = 0.7252$). Therefore, these results indicate amplicon-based whole transcriptome sequencing is a viable tool for profiling samples isolated from our functionalized GO chip.

CTC concentrations (enumeration) associate with tumor burden at blood draw and overall survival

Using the optimized workflow, we then analyzed CTC profiles from a pilot cohort of 15 BC patients, including 14 metastatic BC patients and 1 non-muscle invasive bladder cancer (NMIBC) patient. Within this cohort, 9 patients received pembrolizumab (a PD-1 checkpoint blockade immunotherapy), 14 patients had single time point blood draws, and one patient recorded blood draws at two sequential time points (Fig. 2**A**).

11 of the metastatic BC patients had radiographically visible disease at the time of blood draw and 3 patients had no radiographic evidence of tumor at the time of the draw. We first sought to compare CTCs per mL based on presence or absence of radiographic metastatic disease at the time of blood draw (Fig. 2**B**). In addition, 4 control samples from healthy blood were processed using the same protocol to serve as a negative control. Previous studies looking at CTCs in breast cancer and pancreatic cancer, respectively, have shown that circulating epithelial cells have been identified in the blood of healthy patients [32]. Epithelial cells significantly express both target markers (EPCAM, EGFR), therefore, we believe that cells identified by the microfluidic chip in healthy patients are likely low numbers of circulating epithelial cells. Significantly higher CTC numbers were found in patients with radiographic metastatic disease (mean = 11, CTCs per mL, p-val = 0.0471). We then compared the CTCs per mL between the different blood draw times with respect to their systemic treatments among the metastatic MIBC patients (N = 14). In this cohort, 3 samples were drawn before the patient received systemic treatments, while 6 were drawn during systemic treatment (including 2 samples from one patient drawn at different times during therapy), and 5 were drawn after treatment was completed (Fig. 2**A**). One patient was excluded from this analysis due to lack of follow up. As shown in Fig. 2**C**, no significant difference in CTC concentration was found between the different treatment time points. Overall survival from the time of blood draw and CTC measurement was then analyzed to determine the implication of CTC concentration for patient survival. Next, we sought to divide the patient cohort into high- and low-CTC groups. The maximally selected rank statistic was utilized to determine the effective cut-point at differentiating the high- and low- groups by survival, which yielded an optimal cut-off of ≥ 2.5 CTCs per mL [33]. This cut-off is concordant with previous studies looking at CTCs in prostate cancer that sought to separate patient cohorts into high and low CTC groups based on CTC/mL cutoff's ranging from ≥ 2 to ≥ 5 [34]. As shown in Fig. 2**D**, patients with >2.5 CTCs per mL had significantly shorter overall survival time (p-val = 0.0093). To confirm this association is real, and we were not simply selecting for patients with high disease burden, verses, no evidence of disease, the same analysis was repeated for only the 10 patients whose blood samples were collected prior to treatment, that had a partial/no response to treatment, or that were stable and responding to treatment but still had evidence of disease. Using the same cutoff, patients with >2.5 CTCs per mL trended toward reduced survival (p-val = 0.23) (**Fig. S1**). The Cox regression comparing these two groups yielded a hazard ratio of 3.365 (p-val = 0.26). A power analysis indicates that in order to obtain a significant difference in survival at the estimated hazard ratio between the high- and low- CTC groups, at alpha = 0.05, and with 80 % power, 38 high-CTC samples and 16 low-CTC samples are needed. Although these results are limited by the number of samples, taken together these results indicate that numbers of CTCs enumerated from our GO chip corresponded to overall disease burden and that higher numbers of CTCs may correlate with worse patient survival.

Table 1A
Percentages of invasive marker positive CTCs.

% patients had at least 1 CTC stained positive for	
ADAM15	46.7 %
CD31	58.3 %
EGFR	66.7 %
HER2	16.7 %
% patients had at least 1 CTC stained positive for two markers	58.3 %

Correlation of CTCs with invasive marker expression and overall survival

Because ADAM15, CD31, EGFR, and HER2 are associated with increased tumor invasion and metastatic spread, each was evaluated in isolated CTCs from BC patient samples, summarized in **Table S1**. Examples of immunofluorescent staining images are shown in Fig. 3**A, B**. Following CTC capture, we analyzed the immunofluorescent staining of these biomarkers in selected patients (12 patients for EGFR and HER2, 15 patients for ADAM15) and summarized them in Table 1A. With some patient samples, low numbers of captured cells led to poor image quality (i.e. ADAM15) when evaluating multiple markers. Enumeration of ADAM15+ CTCs from a small subset of patients with metastatic relapse can be found in **Fig. S2.**

We next correlated the CTC expression profiles with overall survival data (Fig. 3**C**). Although the comparison did not reach statistical significance due to limited sample size, patients who had ADAM15+, EGFR+, or HER2+ CTCs trended toward reduced overall survival. These results corroborate with previous literature showing that these markers are associated with tumor progression [17,22,23,35,36]. Overall, our data suggests a possible relationship between these invasive CTC markers and BC patient outcome that should be verified in larger cohorts.

Metastasis related RNA signatures found in patients with high tumor burden and high CTC counts

To further investigate CTC expression signatures in the RNA, amplicon-based targeted RNA sequencing was performed on a total of 13 patient samples, 7 cell line spikes, and 4 healthy controls. The results were analyzed using a custom pipeline, shown in Fig. 4**A**. In short, the read count table was exported from the TorrentSuite software and imported into the R programming language. We then performed normalization, quality control, and unsupervised clustering. To determine if we could detect tumor specific gene signatures from isolated CTC samples, we compared the gene expression profiles from clinical samples with BC cell lines isolated from PBS or spiked into blood. As shown from a principal component analysis (PCA) in Fig. 4**B**, the expression profiles clustered by the presence or absence of blood. This may be a result, in part, of non-tumor RNA in the CTC samples isolated from blood (upper panel) or simply a consequence of the large sample-to-sample heterogeneity. When we specifically compared the RNA signatures of clinical samples (in the lower panel), with patients showing no radiographic evidence of disease, we found a small overlap, but for the most part, good separation between these groups. Additionally, CTC RNA signatures from patients with more significant disease burden clustered separately. In summary, we found a lot of variances within a given cluster due to patient heterogeneity. To correct for patient-to-patient noise, the RUVg method from the RUVseq R package was utilized to estimate and remove factors of variance not attributed to our primary comparison using 84 WBC control genes that should not be differential

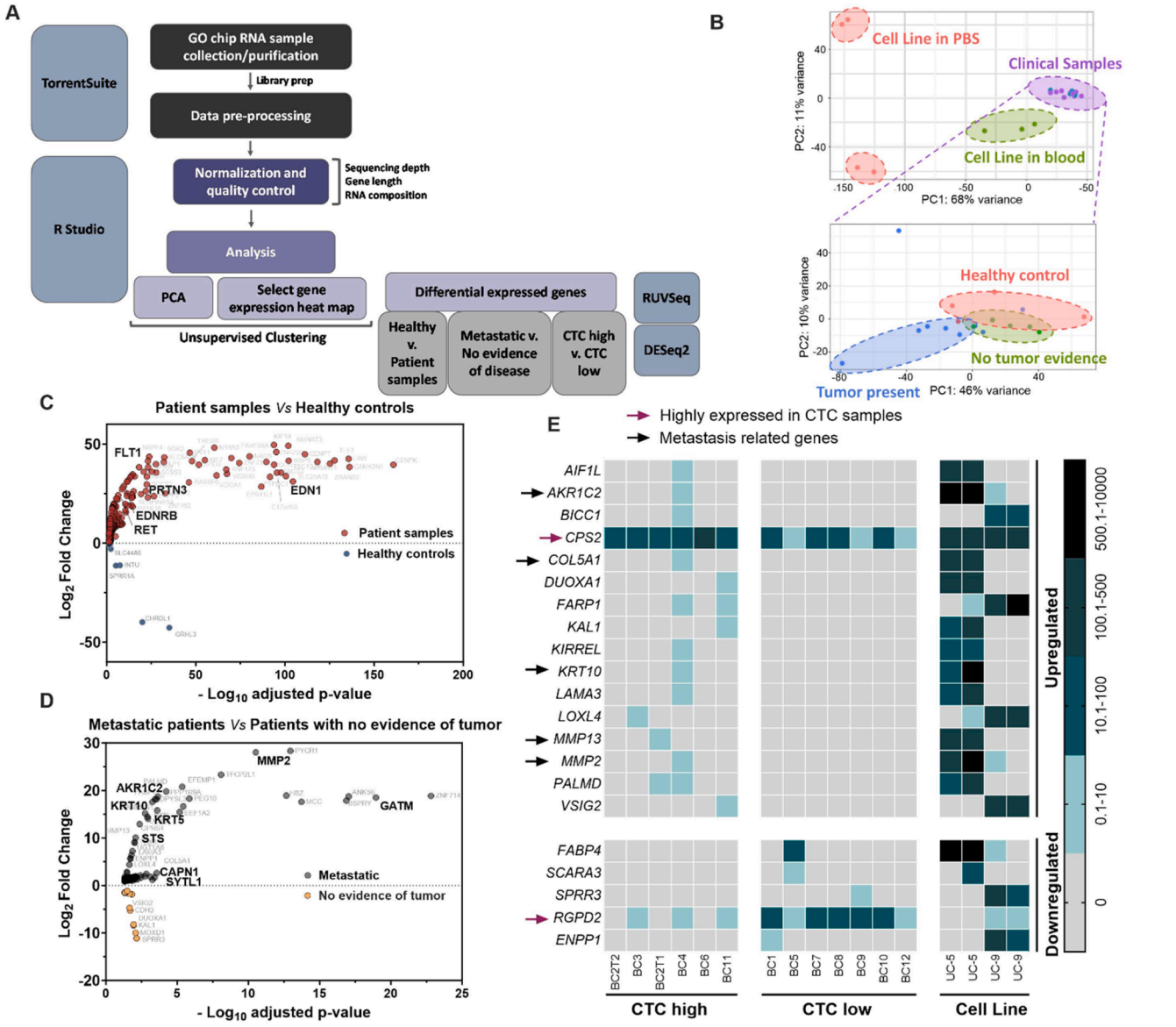

Fig. 4. RNA expression analysis from CTC samples. (A) RNA analysis workflow overview. (B) Principal component analysis (PCA) for the RNA expressions. (C) Volcano plot of significantly differentially expressed genes between patient samples (N = 13) and healthy controls (N = 4). (D) Volcano plot of significantly differentially expressed genes between patients with metastatic disease (N = 8) and patients with no evidence of disease at the time of blood draw (N = 5). (E) Normalized counts using DESeq2 of the differentially expressed genes between patients who have high and low CTC counts (cutoff of 2.5 CTCs per mL).

Table 1B
Top 3 cancer related disease ontologies and their relevant differentially expressed genes between cancer patient and healthy controls.

DISEASE ONTOLOGY	RELEVANT GENES
Urinary System Cancer	FLT1, EDN1, EDNRB, PRTN3, RET, APOE, APOC1, ID1, ALOX5, CDKN1B
Kidney Cancer	FLT1, EDN1, EDNRB, PRTN3, RET, APOE, APOC1, ALOX5, CDKN1B
Prostate Cancer	FLT1, BUB1B, APOE, NR1H3, HSPG2, ID1, CDKN1B

across samples. We next performed differential gene expression analysis and discovered tumor-related traits within isolated CTCs. The differential gene expression profiles were examined by performing 3 separate analyses of the total cohort: (1) healthy controls or patient samples; () patients with and without radiographic metastatic disease; (3) patients who have CTCs > 2.5 per mL and ≤ 2.5 per mL.

Between the CTCs quantified in patient samples (N = 13) and the circulating epithelial cells quantified in healthy controls (N = 4), 216 genes were found to be significantly differentially expressed (adjusted p-val < 0.05, Fold change > 1.5), including 199 upregulated and 17 downregulated genes (Fig. 4**C**). Many genes amongst the 199 enriched genes in CTC samples have been shown to be associated with cancer development. Further bioinformatic analysis reveals enriched cancer ontologies, with 10 genes being strongly associated with genitourinary (GU) system cancer (Table 1B). For example, highly upregulated gene FLT1 (Fms-related tyrosine kinase 1), the receptor of VEGF (Vascular endothelial growth factor), is have been shown in 40 % of urinary bladder cancer patients [37].

As shown in Fig. 4**D**, the comparison between patients with radiographic metastatic tumor (N = 8) and patients with no radiographic disease evidence (N = 5) resulted in 211 differentially expressed genes (adjusted p-val < 0.05, Fold change > 1.5), 197 of which were upregulated in patients with metastatic disease. Interestingly, there were only two common genes (MOXD1 and WDHD1) between this set of

differentially expressed genes (DEGs) and previous DEGs between patient samples and healthy controls indicating potentially unique molecular traits associated with metastasis. Matrix metalloproteinase-2 (MMP-2) is overexpressed in patients with high metastatic burden, and MMP-2 contributes to almost every key step in the metastatic cascade, including epithelial to mesenchymal transition (EMT), cancer cell survival, proliferation, and vascular intravasation [38]. Overexpression of AKR1C2 has been shown to aid the development of cisplatin-based chemoresistance and is a potential high-risk factor in BC patients [39, 40]. Steroid sulfatase (STS) is a steroid sulfate activation enzyme in the androgen signaling pathway known to associate with aggressive tumor characteristics [41]. In BC patients, STS has been shown to promote the invasion capability through the regulation of EMT [42]. Moreover, KRT5 and KRT10 were found to be highly upregulated in the metastatic patient group. These two genes are often found in the basal subtype of BC cell lines, which demonstrate aggressive phenotypes as well [43]. K10 is also thought to act on the retinoblastoma (b) pathway to inhibit proliferation and support EMT progression and metastasis [44]. Additionally, our data identified other examples of well-studied metastasis-related markers including GATM [45], SYTL1 [46], and CAPN1 [47].

We then interrogated the differential expression between patients with high (N = 6) or low (N = 7) CTC enumerations, with a cutoff of 2.5 CTCs per mL. There were 21 DEGs between these two groups, as shown in Fig. 4**E**. Several genes related to metastasis including COL5A1, MMP2, MMP13, AKR1C2, and KRT10, were detected in some samples within the high concentration CTC group. Although the detection of these genes was sparse among the tested samples, some universally expressed genes such as Carbamoyl-Phosphate Synthetase 2 (CAD or CPS2) and RANBP2-like and GRIP domain-containing protein 2 (RGPD2) showed interesting trends. CAD /CPS2 was highly expressed in CTC enriched samples, as well as the cell line controls. CAD/CPS2 is involved in pyrimidine biosynthesis and is upregulated in cancer cells [48]. RGPD2, on the other hand, was highly expressed in several CTC low samples, but not in samples containing high numbers of CTCs, nor in BC cell line controls. RGPD2, though not well studied, demonstrated enriched expression in regulatory T cells. Taken together, these results establish that our CTC capture and RNA profiling platform is capable of high sensitivity transcriptomic analysis within small numbers of BC CTCs in metastatic patients.

Discussion

Molecular profiling of cancer cells is essential to the therapeutic approach of personalized treatments for cancer patients. CTCs hold the promise to ultimately improve personalized medicine through pathological *and* transcriptomic analysis. This novel approach allows for more frequent non-invasive monitoring of disease status, with the hope of improved patient quality of life and improved survival. Until now, BC CTC analysis has been hindered by low detection rate and limited ability to perform molecular profiling analysis. Herein, we present proof-of-concept data, establishing that a highly sensitive GO microfluidic device can be used to enumerate CTCs and examine both protein and RNA in BC CTCs. This initial study tested a two-fold workflow on a limited cohort of 16 BC patients and 5 healthy control samples, where we successfully detected CTCs from all BC patient samples. The CTC concentrations in patients with radiographic evidence of metastatic disease were significantly higher than those in healthy controls and, in patients with no radiographic disease evidence. Additionally, we determined that patients with CTC concentrations higher than 2.5 CTCs per mL had shorter overall survival time. These results are consistent with other published literature in which CTC numbers determined a proxy for disease burden and thus, patient prognosis [8,10,49].

We utilized multiplex immunofluorescent staining to investigate a new set of expression markers, EGFR, HER2, CD31, and ADAM15 on isolated CTCs. We hypothesized that the expression of these additional markers would represent an aggressive CTC subtype, responsible for vascular invasion, and contribute to a worse disease outcome. Although our analysis was limited by sample size, we compared the survival data for the patients with, and without invasive markers, we found that BC patients who expressed ADAM15+, EGFR+, and HER2+ with increased CTC numbers, demonstrated the shortest overall survival trends based on immunostaining.

To elucidate the molecular transcriptomic profiles of CTCs in this same patient population, we developed a workflow utilizing amplicon-based targeted transcriptome sequencing and bioinformatics methods to profile DEGs from bulk RNA material in isolated CTCs. Since patient heterogeneity and technical noise were clouding signatures, we used a set of 84 WBC marker genes to remove unwanted variance not associated with our comparison of interest in these bulk samples. We identified DEGs between; cancer patients and healthy controls; metastatic patients and patients with no radiographic disease evidence, and additionally; patients with high CTC counts and low CTC counts. Many documented metastasis-related gene signatures (KRT5, KRT10, MMP-2, MMP-13, AKR1C2, GATM, SYTL1, and CAPN1) were found to be upregulated in metastatic patient samples. Future studies will investigate expression of genes in CTCs using single cell-based profiling approach to confirm and further this research.

Conclusion

In short, our study establishes the feasibility of combining technologies to broaden the CTC research landscape, while offering a non-invasive, patient-tailored approach to analyze and monitor BC. We recognize that larger cohorts are needed to continue to validate our CTC enumeration cutoff and determine the durability and value of our potential biomarker subset for BC patient prognosis. Likewise, new studies will be important to validate the prognostic value of the markers we identified through transcriptomic analysis of BC CTCs. Incorporation of this technology into larger studies might allow us to de-escalate therapies in those with minimal residual CTCs following therapy and, additionally, to target therapies based on gene expression or protein markers associated with therapeutic responses (i.e. HER2- Pertuzumab and PDL1- immunotherapy).

Methods

Cell culture

BT474, UM-UC-5, UM-UC-9, and UM-UC-18 cell lines were maintained in DMEM (Gibco) with 10 % fetal bovine serum (Sigma) and 1 % antibiotic-antimycotic (Gibco) at 37°C and 5 % CO_2. HUVEC cell line was maintained in complete endothelial cell growth medium (Sigma). Cell lines were routinely tested and reported negative for mycoplasma contamination (Lonza). Western analysis confirmed the expression of ADAM15, HER2, and EGFR in these bladder cell lines [50].

GO chip fabrication and functionalization

The GO chip was fabricated and functionalized as described previously [51]. In brief, a chrome layer (100 Å) and gold layer (1000 Å) were first deposited onto the silicon dioxide wafer. A layer of positive photoresist (SPR 220) was then coated and exposed to UV light under the mask with designed patterns. The patterns formed on the photoresist when immersed in developing reagents, and patterns were then etched into the gold and chrome layer. The photoresist was then removed entirely, and the devices were cut to the correct sizes.

To functionalize, GO suspension was prepared with graphene oxide (GO) nanosheets, N, N-dimethylformamide (DMF), tetrabutylammonium (TBA) hydroxide, and phospholipid-polyethylene–glycol-amine (PL-PEG-NH2). Silicon substrates were immersed in a GO suspension for 10 minutes. The silicon chips underwent sequential washing steps

involving deionized (DI) water, isopropyl alcohol (IPA), and subsequent drying. The silicon substrates and polydimethylsiloxane (PDMS) microfluidic chambers were bonded utilizing corona plasma discharge. The cross-linking agent N-(gamma-maleimidobutyryloxy) succinimide (GMBS) was introduced to the microfluidic chambers and incubated for 30 min. Post-incubation, the chips were washed extensively with ethanol and underwent assembly with tubing. Neutravidin was then actively introduced into the microfluidic devices through syringe pumps, following which the assembled devices were stored at 4 °C until the commencement of sample processing. To prepare chips for processing samples, 1 mL PBS was first run through the device at 100 μL/min to wash off the residual Neutravidin. Then, the antibody cocktail containing 20 μg/mL anti-EpCAM and 20 μg/mL anti-EGFR was processed through the device inlet at 20 μL/min and incubated for 30 min. The antibody cocktail was then run through the outlet with the same incubation to ensure even antibody coating. 3 % bovine serum albumin solution was then processed through the device at 100 μL/min to prevent non-specific binding of WBCs.

Patient selection and approval

The experimental protocol was approved by the Ethics (Institutional Review Board) and Scientific Review Committees of the University of Michigan. All patients gave their informed consent to participate in the study (HUM00041153). Following IRB approval, metastatic bladder cancer patients were identified and provided informed consent. Out of the selected 13 patients (N = 13), five patients previously had metastases but had an excellent response to therapy and thus had no evidence of disease on imaging at the time of blood collection (N = 5). The remaining eight patients had visible metastatic disease (N = 8). Healthy control volunteers (N = 4) consented to participate.

Patient sample collection and CTC isolation from blood

For each patient sample, three GO chips were processed in parallel to perform immunofluorescence (two GO chips) and RNA extraction (one GO chip) within 4 h post-blood draw. In short, 1 mL of blood sample was processed through the GO device at 1 mL/hr following the capturing antibody incubation and BSA incubation as described above. 6 mL of PBS was processed at 100 μL/min to wash off any unbound, non-specific blood cells. Fixation with 1 mL of 4 % paraformaldehyde (PFA) was performed.

Cancer cell isolation from control samples and capture efficiency calculation

Targeted bladder cell lines (UM-UC- 5, UM-UC-9, or UM-UC-18) were pre-labeled with fluorescent green tracker dye (CellTrackerTM Green CMFDA) and counted before being added to PBS or blood. Cell capture was performed by flowing the model samples through the devices at a flow rate of 1 mL/hr. The cells were then fixed in 4 % PFA and permeabilized with 0.2 % Triton-X100 on the chip, followed by nuclear staining with DAPI (4′, 6-diamidino-2-phenylindole). The chips were then scanned using fluorescence microscopy, and the capture efficiency was calculated using the following equation:

$$\text{capture efficiency } (\%) = \frac{\text{cell number captured on chip}}{\text{total cell number processed}} \times 100\%$$

Immunofluorescent staining and CTC identification

Following 4 % PFA fixation and a 6 mL PBS wash, the isolated CTCs from patients were permeabilized using 0.2 % Triton-X100 (Sigma-Aldrich) and incubated for 30 min. The GO devices were then washed with 2 mL PBS and blocked for 30 min with 2 % goat serum (ThermoFisher) plus 3 % BSA to prevent nonspecific staining. The staining antibodies were diluted in 1 % BSA and run through the devices at 50 μL/min and incubated at 4 °C overnight. The following day, 2 mL PBS was run through the two devices at 100 μL/min to wash off excess primary antibodies. The secondary antibodies were prepared, run through the two devices, and incubated for 1.5 h. 2 mL of PBS were again run to wash off excess secondary antibodies. DAPI was then run through the device, incubated 15 min, washed off using 1 mL of PBS. Finally, the devices were scanned and analyzed using Nikon Ti2 fluorescent microscope and the Nikon-Elements software. A summary of the antibody products used is shown in Table 2A.

Table 2A
Summary of antibodies used for the 2 staining panels.

Marker	Primary antibody	Secondary antibody	Staining Panels
CD45	Santa Cruz Sc-70699	Thermofisher A11006	Panel 1 & 2
CK7/8	BD 349205	Thermofisher A21133	Panel 1 & 2
EGFR	Thermofisher 2800005	Thermofisher A21240	Panel 1
HER2	Cell Signaling 2165	Thermofisher SA5-10035	Panel 1
CD31	R&D Systems BBA7	Thermofisher A21240	Panel 2
ADAM15	Novopro 101503	Thermofisher SA5-10035	Panel 2

CTCs were identified as DAPI+/CK7/8+/CD45- based on the staining images. Of these identified CTCs, expression of invasive markers was recorded as binary variables for further analysis.

RNA extraction and targeted whole-transcriptome sequencing

RNA extraction was performed on the third GO chip parallel device after 1 ml blood sample processing and a PBS washing step. In short, 100 μL Arcturus® PicoPure® RNA Extraction buffer (Life Technologies) was run through the device at 3 mL/hr. The device was then incubated at 42 °C for 30 min. Following incubation, 100 μL ultrapure DNAase-free and RNAase free DEPC water Fischer® was run through the device, and the effluent materials were collected. These materials were purified using Arcturus® PicoPure® RNA Isolation Kit according to the manufacturer's instructions. The resulting 11 μL of purified RNA was stored at -80 °C until the library was prepared.

We performed amplicon-based whole-transcriptome sequencing using the Ion Ampliseq Transcriptome Human Gene Expression Kit (Life Technologies) according to the manufacturer's instructions with approximately 0.3 ng of RNA per sample, allowing for interrogation of ~21,000 RNA transcripts. Library preparation was performed according to the manufacturer's instructions. Technical replicate libraries and templates were independently constructed and sequenced on separate chips. Reads were mapped and quantified using version 5.16.1 of TorrentSuite's (Life Science Technologies) Coverage Analysis plugin with the default parameters.

Bioinformatics analysis and removing unwanted variance

The read count table was exported into the R programming language for further analysis. We first filtered out any genes that did not have 5 or more reads in at least two patient samples. Normalization was performed using the upper-quartile method in the EDASeq package followed by PCA [52,53]. We then used the RUVg method from the RUVseq R package to eliminate unwanted variation not attributed to our variable of interest, according to the published workflow [54]. Two input parameters were needed: a set of negative control genes and the factor number, k. Since WBCs are not perturbed in this analysis, their associated genes were selected as negative controls since it is expected that there is no difference in expression across samples. For the negative control genes, we first selected a broad range of 1746 leukocyte marker genes from available databases [55,56], and then filtered this list down to genes most expressed in our experiment. To do this, we first plotted the average expression and standard deviation of these 1746 genes within the healthy control and cell line samples using a density plot

Table 2B
Density plots for selected WBC-related genes and criteria for selecting relevant WBC control genes.

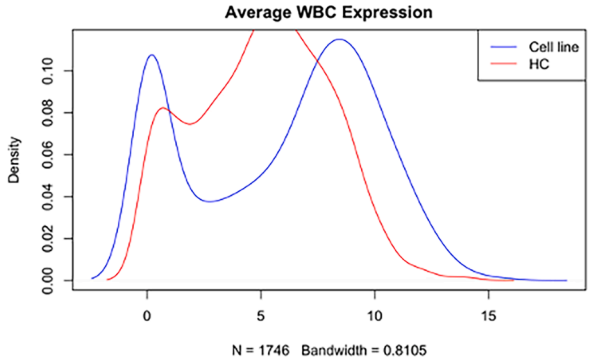

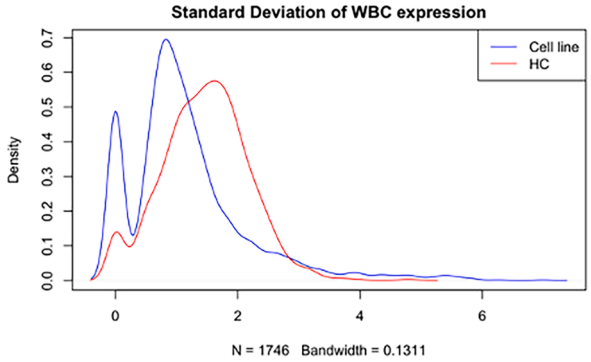

Select genes whose average log expression is:	Select genes whose standard deviation is:
> 5 within all HC samples	> 1.5 within all HC samples
< 4 within all Cell line samples	< 0.6 within all Cell line samples

(shown in Table 2B). We then set a series of criteria to find genes both highly expressed in processed healthy blood control samples and lowly expressed in our cell line control samples. The detailed selection criteria are listed in Table 2B.

Using this criteria, 84 WBC marker genes were selected as negative control genes. For the factor number k, we experimented with k equals 1 to 5 based on the small patient sample size [54,57]. The resulting differential gene expression did not seem to be affected by the k number. We chose k equals 2 as the input parameter. After normalization, DESeq2 was used to perform differential expression analysis. A given gene was considered differentially expressed if its false discovery rate (FDR) corrected p-value was <0.05 and its absolute fold change >1.5. Pathway analysis was performed using the identified DEGs and the ClusterProfiler package [58,59].

Statistical analysis

Statistical analysis was conducted in GraphPad Prism V9 and the R programming language. Comparisons of CTC numbers between two groups were performed using unpaired Student's t-tests, two-tailed. Survival analysis was performed using Kaplan-Meier survival curves with the Log-rank method (Mantel-Cox test) in GraphPad Prism. Power analysis was performed using the powerSurvEpi R package. The last follow up date for patient samples was April 22nd, 2022. For RNA analysis, correlation was performed using simple linear regression in R, and the coefficient of determination, R^2, was reported.

Funding

This work was supported in part by the NIH awards to S. Nagrath and the Rogel Cancer Center: [R33CA202867], [R01CA208335], [U01CA210152]; and awards to P.L. Palmbos: NIH [R37CA273138] and Damon Runyon Clinical Investigator Award. Additional funding to Rogel Comprehensive Cancer Center: NIH [P30CA046592], for use of Biostatistics, Analytics, and Bioinformatics Shared Resources.

CRediT authorship contribution statement

Zeqi Niu: Validation, Software, Methodology, Formal analysis, Data curation, Conceptualization. **Molly Kozminsky:** Validation, Software, Methodology, Formal analysis, Data curation, Conceptualization. **Kathleen C. Day:** Writing – review & editing, Writing – original draft, Validation, Project administration, Investigation, Data curation, Conceptualization. **Luke J. Broses:** Validation, Methodology, Investigation, Data curation. **Marian L. Henderson:** Writing – review & editing, Visualization, Validation. **Christopher Patsalis:** Writing – review & editing, Validation, Software, Formal analysis, Data curation. **Rebecca Tagett:** Software, Methodology, Formal analysis, Data curation. **Zhaoping Qin:** Methodology, Data curation. **Sarah Blumberg:** Software, Methodology. **Zachery R. Reichert:** Validation, Resources, Data curation. **Sofia D. Merajver:** Funding acquisition. **Aaron M. Udager:** Software, Resources, Methodology, Formal analysis, Data curation, Conceptualization. **Phillip L. Palmbos:** Writing – review & editing, Validation, Resources, Methodology, Funding acquisition, Data curation. **Sunitha Nagrath:** Writing – original draft, Visualization, Validation, Supervision, Software, Resources, Project administration, Methodology, Investigation, Funding acquisition, Formal analysis, Data curation, Conceptualization. **Mark L. Day:** Writing – review & editing, Writing – original draft, Validation, Supervision, Resources, Project administration, Methodology, Funding acquisition, Formal analysis, Data curation, Conceptualization.

Declaration of competing interest

The authors declare that they have no known competing financial interests or personal relationships that could have appeared to influence the work reported in this paper.

Supplementary materials

Supplementary material associated with this article can be found, in the online version, at doi:10.1016/j.neo.2024.101036.

References

[1] Anon. World cancer research day 2023: the bladder cancer epidemiology and early detection in Africa (BEED) study [Internet]. [cited 2024 Jan 16]. Available from: https://www.iarc.who.int/cancer-type/bladder-cancer.
[2] Anon. Institute NC. Surveillance, epidemiology, and end results (SEER) program SEER*Stat database: cancer stat facts: bladder cancer [Internet]. 2022. Available from: www.seer.cancer.gov.
[3] J.A. Witjes, H.M. Bruins, R. Cathomas, E.M. Compérat, N.C. Cowan, G. Gakis, et al., European association of urology guidelines on muscle-invasive and metastatic bladder cancer: summary of the 2020 guidelines, Eur. Urol. 79 (1) (2021) 82–104.
[4] J.J. Meeks, H. Al-Ahmadie, B.M. Faltas, J.A. Taylor, T.W. Flaig, D.J. DeGraff, et al., Genomic heterogeneity in bladder cancer: challenges and possible solutions to improve outcomes, Nat. Rev. Urol. 17 (5) (2020) 259–270.
[5] A.G. Robertson, J. Kim, H. Al-Ahmadie, J. Bellmunt, G. Guo, A.D. Cherniack, et al., Comprehensive molecular characterization of muscle-invasive bladder cancer, Cell 171 (3) (2017) 540–556 [Internet]Oct 19 [cited 2024 Jun 20]e25Available from, https://www.sciencedirect.com/science/article/pii/S0092867417310565.
[6] Y. Wang, T.H. Kim, S. Fouladdel, Z. Zhang, P. Soni, A. Qin, et al., PD-L1 expression in circulating tumor cells increases during radio(chemo)therapy and indicates poor prognosis in non-small, Cell Lung Cancer Sci Rep. 9 (1) (2019) 566.

[7] S. Pang, H. Li, S. Xu, L. Feng, X. Ma, Y. Chu, et al., Circulating tumour cells at baseline and late phase of treatment provide prognostic value in breast cancer, Sci. Rep. 11 (1) (2021) 13441.

[8] W.A. Cieślikowski, A. Antczak, M. Nowicki, M. Zabel, J. Budna-Tukan, Clinical relevance of circulating tumor cells in prostate cancer management, Biomedicines 9 (2021).

[9] P. Gazzaniga, A. Gradilone, E. De berardinis, G.M. Busetto, C. Raimondi, O. Gandini, et al., Prognostic value of circulating tumor cellsin nonmuscle invasive bladder cancer: Acellsearch analysis, Ann. Oncol. 23 (9) (2012) 2352–2356.

[10] E. Fina, A. Necchi, P. Giannatempo, M. Colecchia, D. Raggi, M.G. Daidone, et al., Clinical significance of early changes in circulating tumor cells from patients receiving first-line cisplatin-based chemotherapy for metastatic urothelial carcinoma, Bladder Cancer 2 (4) (2016) 395–403.

[11] B. Rupp, H. Ball, F. Wuchu, D. Nagrath, S. Nagrath, Circulating tumor cells in precision medicine: challenges and opportunities, Trends Pharmacol. Sci. 43 (5) (2022) 378–391.

[12] S.J. Cheng, K.Y. Hsieh, S.L. Chen, C.Y. Chen, C.Y. Huang, H.I. Tsou, et al., Microfluidics and nanomaterial-based technologies for circulating tumor cell isolation and detection, Sensors 20 (2020).

[13] H.J. Yoon, T.H. Kim, Z. Zhang, E. Azizi, T.M. Pham, C. Paoletti, et al., Sensitive capture of circulating tumour cells by functionalized graphene oxide nanosheets, Nat. Nanotechnol. 8 (10) (2013) 735–741, 2013/09/29 edOct.

[14] S. Nagrath, L.V. Sequist, S. Maheswaran, D.W. Bell, D. Irimia, L. Ulkus, et al., Isolation of rare circulating tumour cells in cancer patients by microchip technology, Nature 450 (7173) (2007) 1235–1239. Dec 20.

[15] T.H. Kim, H.J. Yoon, S. Fouladdel, Y. Wang, M. Kozminsky, M.L. Burness, et al., Characterizing circulating tumor cells isolated from metastatic breast cancer patients using graphene oxide based microfluidic assay, Adv. Biosyst. 3 (2) (2019) 1800278.

[16] M. Kozminsky, S. Fouladdel, J. Chung, Y. Wang, D.C. Smith, A. Alva, et al., Detection of CTC clusters and a dedifferentiated RNA-expression survival signature in prostate cancer, Adv. Sci. 6 (2) (2019) 1801254.

[17] D.H. Hovelson, A.M. Udager, A.S. McDaniel, P. Grivas, P. Palmbos, S. Tamura, et al., Targeted DNA and RNA sequencing of paired urothelial and squamous bladder cancers reveals discordant genomic and transcriptomic events and unique therapeutic implications, Eur. Urol. 74 (6) (2018) 741–753. Dec.

[18] K.C. Day, G.L. Hiles, M. Kozminsky, S.J. Dawsey, A. Paul, L.J. Broses, et al., HER2 and EGFR overexpression support metastatic progression of prostate cancer to bone, Cancer Res. 77 (1) (2017) 74–85.

[19] M. Rink, F.K. Chun, R. Dahlem, A. Soave, S. Minner, J. Hansen, et al., Prognostic role and HER2 expression of circulating tumor cells in peripheral blood of patients prior to radical cystectomy: a prospective study, Eur. Urol. 61 (4) (2012) 810–817.

[20] S. Ithimakin, K.C. Day, F. Malik, Q. Zen, S.J. Dawsey, T.F. Bersano-Begey, et al., HER2 drives luminal breast cancer stem cells in the absence of HER2 amplification: implications for efficacy of adjuvant trastuzumab, Cancer Res. 73 (5) (2013) 1635–1646.

[21] A. Anantharaman, T. Friedlander, D. Lu, R. Krupa, G. Premasekharan, J. Hough, et al., Programmed death-ligand 1 (PD-L1) characterization of circulating tumor cells (CTCs) in muscle invasive and metastatic bladder cancer patients, BMC Cancer 16 (1) (2016) 744.

[22] G. Lorenzatti Hiles, A. Bucheit, J.R. Rubin, A. Hayward, A.L. Cates, K.C. Day, et al., ADAM15 is functionally associated with the metastatic progression of human bladder cancer, PLoS One 11 (3) (2016) e0150138.

[23] A.J. Najy, K.C. Day, ML. Day, ADAM15 supports prostate cancer metastasis by modulating tumor cell–endothelial cell interaction, Cancer Res. 68 (4) (2008) 1092–1099.

[24] C.E. Gast, A.D. Silk, L. Zarour, L. Riegler, J.G. Burkhart, K.T. Gustafson, et al., Cell fusion potentiates tumor heterogeneity and reveals circulating hybrid cells that correlate with stage and survival, Sci. Adv. 4 (9) (2018). Sep 12eaat7828–eaat7828.

[25] W. Li, Y. Wang, S. Tan, Q. Rao, T. Zhu, G. Huang, et al., Overexpression of epidermal growth factor receptor (EGFR) and HER-2 in bladder carcinoma and its association with patients' clinical features, Med Sci Monit Int Med J Exp Clin Res 24 (2018) 7178–7185. Oct 8.

[26] G. Wishart, A. Templeman, F. Hendry, K. Miller, A.S. Pailhes-Jimenez, Molecular profiling of circulating tumour cells and circulating tumour DNA: complementary insights from a single blood sample utilising the parsortix® system, Curr. Issues Mol. Biol. 46 (1) (2024) 773–787 [Internet]Jan 17 [cited 2024 Feb 7]Available from, https://www.ncbi.nlm.nih.gov/pmc/articles/PMC10814787/.

[27] E.O.T. Chan, V.W.S. Chan, J.Y.T. Poon, B.H.K. Chan, C.P. Yu, P.K.F. Chiu, et al., Clear cell carcinoma of the urinary bladder: a systematic review, Int. Urol. Nephrol. 53 (5) (2021) 815–824, https://doi.org/10.1007/s11255-020-02725-2 [Internet] May 1 [cited 2024 Feb 7]Available from.

[28] C.V. Pecot, F.Z. Bischoff, J.A. Mayer, K.L. Wong, T. Pham, J. Bottsford-Miller, et al., A novel platform for detection of CK+ and CK− CTCs, Cancer Discov. 1 (7) (2011) 580–586, https://doi.org/10.1158/2159-8290.CD-11-0215 [Internet].Dec 13 [cited 2024 Feb 7]Available from.

[29] A. Awadalla, H. Abol-Enein, M.M. Gabr, E.T. Hamam, AA. Shokeir, Prediction of recurrence and progression in patients with T1G3 bladder cancer by gene expression of circulating tumor cells, Urol. Oncol. Semin. Orig. Investig. 38 (4) (2020) 278–285.

[30] P. Gazzaniga, I. Nofroni, O. Gandini, I. Silvestri, L. Frati, A.M. Aglianò, et al., Tenascin C and epidermal growth factor receptor as markers of circulating tumoral cells in bladder and colon cancer, Oncol. Rep. 14 (5) (2005) 1199–1202.

[31] FA.W Coumans, C.J.M. Doggen, G. Attard, J.S. de Bono, L. Terstappen, All circulating EpCAM+CK+CD45- objects predict overall survival in castration-resistant prostate cancer, Ann. Oncol. Off. J. Eur. Soc. Med. Oncol. 21 (9) (2010) 1851–1857. Sep.

[32] A.E. Ring, L. Zabaglo, M.G. Ormerod, I.E. Smith, M. Dowsett, Detection of circulating epithelial cells in the blood of patients with breast cancer: comparison of three techniques, Br. J. Cancer 92 (5) (2005) 906–912 [Internet]Mar [cited 2024 Jul 9]Available from, https://www.nature.com/articles/6602418.

[33] T. Hothorn, A. Zeileis, Generalized maximally selected statistics, Biometrics 64 (4) (2008) 1263–1269, https://doi.org/10.1111/j.1541-0420.2008.00995.x [Internet] Dec 1 [cited 2024 Jun 19]Available from.

[34] Z.R. Reichert, T. Kasputis, S. Nallandhighal, S.M. Abusamra, A. Kasputis, S. Haruray, et al., Multigene profiling of circulating tumor cells (CTCs) for prognostic assessment in treatment-naïve metastatic hormone-sensitive prostate cancer (mHSPC), Int. J. Mol. Sci. 23 (1) (2021) 4 [Internet].Dec 21 [cited 2024 Jul 9]Available from, https://www.ncbi.nlm.nih.gov/pmc/articles/PMC8744626/.

[35] N. Lucas, A.J. Najy, M.L. Day, The therapeutic potential of ADAM15, Curr. Pharm. Des. 15 (20) (2009) 2311–2318.

[36] K.P.S. Raghav, M.M. Moasser, Molecular pathways and mechanisms of HER2 in cancer therapy, Clin. Cancer Res. Off. J. Am. Assoc. Cancer Res. 29 (13) (2023) 2351–2361. Jul 5.

[37] K. Sato, R. Sasaki, Y. Ogura, N. Shimoda, H. Togashi, K. Terada, et al., Expression of vascular endothelial growth factor gene and its receptor (flt-1) gene in urinary bladder cancer, Tohoku J. Exp. Med. 185 (3) (1998) 173–184. Jul.

[38] M. Tauro, CC. Lynch, Cutting to the chase: How matrix metalloproteinase-2 activity controls breast-cancer-to-bone metastasis, Cancers 10 (6) (2018). . (Basel).

[39] H.L. Tai, T.S. Lin, H.H. Huang, T.Y. Lin, M.C. Chou, S.H. Chiou, et al., Overexpression of aldo-keto reductase 1C2 as a high-risk factor in bladder cancer, Oncol. Rep. 17 (2) (2007) 305–311.

[40] A. Shirato, T. Kikugawa, N. Miura, N. Tanji, N. Takemori, S. Higashiyama, et al., Cisplatin resistance by induction of aldo-keto reductase family 1 member C2 in human bladder cancer cells, Oncol. Lett. 7 (3) (2014) 674–678, 2013/12/19 edMar.

[41] K.M. McNamara, F. Guestini, T. Sauer, J. Touma, I.R. Bukholm, J.C. Lindstrøm, et al., In breast cancer subtypes steroid sulfatase (STS) is associated with less aggressive tumour characteristics, Br. J. Cancer 118 (9) (2018) 1208–1216.

[42] Y. Shimizu, S. Tamada, M. Kato, Y. Takeyama, M. Fujioka, A. Kakehashi, et al., Steroid sulfatase promotes invasion through epithelial-mesenchymal transition and predicts the progression of bladder cancer, Exp. Ther. Med. 16 (6) (2018) 4463–4470.

[43] W. Choi, B. Czerniak, A. Ochoa, X. Su, A. Siefker-Radtke, C. Dinney, et al., Intrinsic basal and luminal subtypes of muscle-invasive bladder cancer, Nat. Rev. Urol. 11 (7) (2014) 400–410. Jul.

[44] Anon. Disruption of Rb/E2F pathway results in increased cyclooxygenase-2 expression and activity in prostate epithelial cells | cancer research | american association for cancer research [Internet]. [cited 2024 Jun 6]. Available from: https://aacrjournals.org/cancerres/article/65/9/3633/519684/Disruption-of-Rb-E2F-Pathway-Results-in-Increased.

[45] L. Zhang, Z. Zhu, H. Yan, W. Wang, Z. Wu, F. Zhang, et al., Creatine promotes cancer metastasis through activation of Smad2/3, Cell Metab. 33 (6) (2021) 1111–1123 [Internet]Jun 1 [cited 2024 Jun 7]e4Available from, https://www.sciencedirect.com/science/article/pii/S1550413121001169.

[46] X. Xu, Y. Wang, S. Zhang, Y. Zhu, J. Wang, Exploration of prognostic biomarkers of muscle-invasive bladder cancer (MIBC) by bioinformatics, Evol. Bioinform. 17 (2021) 11769343211049270.

[47] H. Nian, B. Ma, Calpain-calpastatin system and cancer progression, Biol. Rev. Camb. Philos. Soc. 96 (3) (2021) 961–975. Jun.

[48] T. Aoki, G. Weber, Carbamoyl phosphate synthetase (glutamine-hydrolyzing): increased activity in cancer cells, Science 212 (4493) (1981) 463–465 (1979).

[49] H. Jiang, X. Gu, Z. Zuo, G. Tian, J. Liu, Prognostic value of circulating tumor cells in patients with bladder cancer: A meta-analysis, PLoS One 16 (7 July) (2021) 1–12.

[50] X. Tan, L.J. Broses, M. Zhou, K.C. Day, W. Liu, Z. Li, et al., Multiparameter urine analysis for quantitative bladder cancer surveillance of orthotopic xenografted mice, Lab Chip 20 (3) (2020) 634–646. Feb 7.

[51] H.J. Yoon, A. Shanker, Y. Wang, M. Kozminsky, Q. Jin, N. Palanisamy, et al., Tunable thermal-sensitive polymer–graphene oxide composite for efficient capture and release of viable circulating tumor cells, Adv. Mater. 28 (24) (2016) 4891–4897 [Internet][cited 2024 Jan 16]Available from, https://onlinelibrary.wiley.com/doi/abs/10.1002/adma.201600658.

[52] D. Risso, K. Schwartz, G. Sherlock, S. Dudoit, GC-content normalization for RNA-Seq data, BMC Bioinform. 12 (1) (2011) 480.

[53] J.H. Bullard, E. Purdom, K.D. Hansen, Dudoit S. Evaluation of statistical methods for normalization and differential expression in mRNA-Seq experiments, BMC Bioinform. 11 (1) (2010) 94.

[54] D. Risso, J. Ngai, T.P. Speed, Dudoit S. Normalization of RNA-seq data using factor analysis of control genes or samples, Nat. Biotechnol. 32 (9) (2014) 896–902.

[55] C. Palmer, M. Diehn, A.A. Alizadeh, P.O. Brown, Cell-type specific gene expression profiles of leukocytes in human peripheral blood, BMC Genom. 7 (1) (2006) 115.
[56] X. Xie, M. Liu, Y. Zhang, B. Wang, C. Zhu, C. Wang, et al., Single-cell transcriptomic landscape of human blood cells, Natl. Sci. Rev. 8 (3) (2021) nwaa180.
[57] J.A. Gagnon-Bartsch, TP. Speed, Using control genes to correct for unwanted variation in microarray data, Biostatistics 13 (3) (2012) 539–552.
[58] G. Yu, L.G. Wang, G.R. Yan, QY. He, DOSE: an R/Bioconductor package for disease ontology semantic and enrichment analysis, Bioinforma Oxf. Engl. 31 (4) (2015) 608–609. Feb 15.
[59] G. Yu, L.G. Wang, Y. Han, QY. He, clusterProfiler: an R package for comparing biological themes among gene clusters, OMICS J. Integr. Biol. 16 (5) (2012) 284–287 [Internet]May [cited 2024 Jan 16]Available from, https://www.ncbi.nlm.nih.gov/pmc/articles/PMC3339379/.